Corrosion behaviour of Fe-Mn-Si-Al austenitic steel in chloride solution

M. Opiela*, A. Grajcar , W. Krukiewicz

Division of Constructional and Special Materials,

Institute of Engineering Materials and Biomaterials,

Silesian University of Technology, ul. Konarskiego 18a, 44-100 Gliwice, Poland

* Corresponding author: E-mail address: marek.opiela@polsl.pl

Properties

ABSTRACT

Purpose: The aim of the paper is to investigate the corrosion behaviour of the new-developed high-manganese austenitic steel in 0.5n NaCl solution.

Design/methodology/approach: The steel used for the investigation was thermomechanically rolled and solution heat-treated from a temperature of 850°C. Corrosion resistance of investigated steel was examined using weight and potentiodynamic methods. In the weight method, the specimens were immersed in the prepared solution for 24h. In the potentiodynamic method, anodic polarization curves with a rate of potential changes of 1 mV/s in the anodic direction were registered. After the current density being equal 1 mA/cm2 was achieved, the direction of polarization has been changed. Basing on the registered curves, the pitting potential, repassivation potential, polarization resistance and corrosion current were determined.

Findings: It was found that the steel is characterized by a partially recrystallized austenitic microstructure with numerous annealing twins and slip bands. According to the results of potentiodynamic analyses it was found that the samples of examined steel show poor corrosion resistance in the NaCl solution. The observed corrosion pits are related to the chemical composition. It is connected with the high dissolution rate of Mn and Fe atoms in NaCl solution. Fractographic analyses of samples revealed corrosion products on their surface in a form of pits with diversified size.

Research limitations/implications: To investigate in more detail the corrosion behaviour of high-manganese steel, the investigations should include steels with a wider Al concentration.

Practical implications: The obtained results can be used for searching the appropriate way of improving the corrosion resistance of a modern group of high-manganese austenitic steels.

Originality/value: The corrosion behaviour in chloride solution of a new-developed Fe-Mn-Si-Al steel was investigated.

Keywords: Corrosion resistance; Thermo-mechanical processing; High-manganese steels; TWIP-effect; Potentiodynamic tests; NaCl solution

Research paper

1. Introduction

Significant progress in a field of development of new groups of steels assigned for sheets in the automotive industry has been made in the period of the last twenty years. From the aspect of materials, this development has been accelerated by strong competition with non-ferrous aluminium and magnesium alloys as well as with composite polymers, which meaning has been successively increasing. From the aspect of ecology, an essential factor is to limit the amount of exhaust gas emitted into the environment. It's strictly connected to fuel consumption, mainly dependent on a car weight. Taking into consideration increased quantity of accessories used in modern cars, reduce of car weight can be achieved solely throughout optimalization of sections of sheets used for bearing and reinforcing elements as well as for body panelling parts of a car. Application of sheets with lower thickness preserving proper stiffness requires application of sheets with higher mechanical properties, however keeping adequate formability. Steels of IF and BH type with moderate mechanical properties and high susceptibility to deep drawing were elaborated for elements of body panelling [1, 2]. However, the widest range of applications belongs to multiphase steels containing martensite islands in a ferritic matrix [3] or bainitic-austenitic [4]. Sheets made of these steels are widely used for bearing and reinforcing elements.

Nowadays, apart from limiting fuel consumption, special pressure is placed on increasing the safety of car users. Constructional solutions and steels used in the frontal part of a vehicle are the most significant due to the possibility of accident occurrence. The role of structural elements such as frontal frame side members, bumpers and other parts is to take over the energy of an impact. Therefore, steels that are used for these parts should be characterized by high product of UTS and UEl, proving the ability of energy absorption. The benefits deriving from taking advantage of cold strain-induced martensitic transformation of retained austenite in TRIP-type steels (TRansformation Induced Plasticity) [5] have captured the attention of materials engineers to steels with homogeneous austenite microstructure. Although TRIP effect can be achieved in Cr-Ni austenitic steels [6], they are too expensive for their application in the automotive industry. Therefore, intense research on high-manganese austenitic steels has been performed in the recent years. Apart from 15÷30%Mn they also contain 0.03÷0.2%C, 1÷3%Si, 1÷3%Al [7]. Mechanical properties of these steels depend on structural processes occurring during cold plastic deformation, which in turn are the derivative of stacking fault energy of austenite [8]. In case it's equal from 12 to 20 mJm^{-2}, a partial transformation of austenite into martensite occurs taking advantage of TRIP effect [9]. Values of SFE equal from 20 to 60 mJm^{-2} determine intense course of mechanical twinning connected to TWIP effect (TWinning Induced Plasticity) [10]. Making use of these phenomena allows shaping mechanical properties of steels in a wide range, i.e. $YS_{0.2}$ = 250÷400 MPa, UTS = 500÷1000 MPa, UEl = 30÷70%. Moreover, strong strain hardening causes that the value of instantaneous hardening exponent is maintained at a high level up to high values of deformation [7]. This beneficial connection of mechanical properties predisposes discussed steels for their application for parts absorbing impact energy, as well as for parts with complex shape, generally fabricated in several operations.

The research conducted at the present is focused mainly on investigation of behaviour of high-manganese steels during cold-working [8-13] or hot-working [14-17]. However, there is still no sufficient information regarding their corrosion resistance. The research [18, 19] of Fe-C-Mn-Al steels for cryogenic applications that were supposed to substitute expensive Cr-Ni steels was carried out in the eighties of the last century. The role of manganese boils to Ni replacement and obtaining austenitic microstructure, whereas aluminium has a similar impact as chromium. Improvement of corrosion resistance by Al consists in formation of thin, stable layer of oxides. In the result of conducted research it was found that Fe-C-Mn-Al steels show inferior corrosion resistance than Cr-Ni steels and they can be used as a substitute only in some applications [19]. Corrosion resistance of Fe-0.5C-29Mn-3.5Al-0.5Si steel in 3.5% NaCl solution has been recently investigated by Ghayad and others [20]. They have found that investigated steel does not yield to passivation independently from the state: supersaturated, aged or strain aged. The steel was subjected to general corrosion, particularly intense after the appearance of the second phase in the form of ferrite, after sustained ageing at the temperature of 550°C. The behaviour of Fe-0.2C-25Mn-8Al steel with increased concentration of aluminium up to 8% wt. in the medium of HNO$_3$ and NaCl has been investigated by Hamada [21], who has found that in the medium of HNO$_3$ solution, the steel with high concentration of Al is covered by a thin layer of salt. After increasing Mn concentration to 30% and introducing additionally 6%Cr, the steel undergoes passivation and is covered by considerably more stable film of oxides. In addition, the steel containing Al and Cr shows resistance to the effects of 3.5% NaCl, that is not present in case of the steel containing only increased concentration of aluminium [22].

The research carried out so far has not taken into account the influence of silicon on a course of corrosion phenomena as well as an influence of Nb and Ti microadditions. Moreover, thermo-mechanical processing conducted in the work and behaviour of investigated steel in the chloride medium may have an essential meaning.

2. Experimental procedure

The research was carried out on high-manganese austenitic steel with a chemical composition presented in Table 1. This type of steels finds repeatedly wider application for different kinds of structural components of vehicles characterized by advantageous connection of strength and ductile properties. This particularly profitable combination of properties has a meaning not only in the production process of steel and car components, but also during possible accident while using the car, because of relatively high reserve of plasticity in the zones of controlled energy absorption of the car being damaged.

Table 1.
Chemical composition of the investigated steel.

Mass contents, (%)				
C	Mn	Si	Al	P
0.054	24.4	3.49	1.64	0.004
S	Nb	Ti	N	O
0.016	0.029	0.079	0.0039	0.0006

The material used for the investigation was delivered in a form of segment of steel sheet with the following dimensions 340x225x3.1 mm, obtained in a rolling process using the thermo-mechanical treatment method. Thermo-mechanical processing of studied steel included:

- heating of a charge up to the temperature of 1150°C,
- austenitizing at the temperature of 1150°C for 15 minutes,
- rolling of the charge in a temperature range from 1050°C to 850°C, according to established conditions (Table 2),
- isothermal holding of a rolled segment of sheet at the temperature of finishing rolling for 15s,
- solution heat treatment of the flats in water.

Table 2.
Rolling schedule for the flats with a thickness of 5.4 mm

Pass number	Deformation temperature, °C	Thickness before the pass, mm	Thickness after the pass, mm	Relative reduction, %
1	1050	5.4	4.3	20
2	950	4.3	3.7	15
3	850	3.7	3.1	15

Corrosion resistance of investigated steel was examined using weight and potentiodynamic methods.

Weight method. Corrosion tests were carried out in 0.5N NaCl solution on samples with 16.9x16.1x3.1 mm dimensions. Specimens were cleaned in 95.6% ethanol and they were weighed on analytical balance before starting the analysis. Temperature of the solution during the test was equal 23ºC±1ºC, whereas the time of the test was equal 24h. Volume of corrosion loss was calculated using the following dependence:

$$V_u = \frac{V_p - V_k}{V_p} \cdot 100\%$$ (1)

where: V_p – initial volume of a sample [mm^3], V_k – volume of a sample after corrosion tests [mm^3].

Corrosion rate was determined basing on the dependence (2):

$$V_{cor} = \frac{\Delta m}{S \cdot t}$$ (2)

where: S – surface of a sample [mm^2], t – time of the measurement [h], Δm – mass loss of a sample [g].

Potentiodynamic method. Corrosion tests were carried out in 0.5N solution of NaCl. Temperature of the solution during the test was equal 23ºC ± 1ºC. Specimens were cleaned in 95.6% ethanol before starting the analysis. Tests were initiated from determination of E_{ocp} open circuit potential and then anodic polarization curves with a rate of potential changes of 1 mV/s in the anodic direction were registered. After the current density being equal 1 mA/cm^2 was achieved, the direction of polarization has been changed. In such way, the return curve was registered. According to registered curves, chemical quantities describing corrosion resistance were determined: pitting potential E_b (mV), repassivation potential E_{cp} (mV) – if occurred, polarization resistance R_p (kΩ·cm^2) and corrosion current i_{cor} (A/cm^2). In order to calculate the corrosion current, the Stern-Geary equation was used [23]:

$$R_p = \frac{b_k \cdot b_a}{2,3 \cdot i_{cor}(b_a + b_k)}$$ (3)

where: b_k – the slope coefficient of the cathodic Tafel line, b_a – the slope coefficient of the anodic Tafel line, i_{cor} – the corrosion current density [mA/cm^2], R_p – the polarization resistance [Ωcm^2].

Microstructure observations of specimens coming from rolled segment of the sheet etched in nital, as well as of those after corrosion tests, were carried out on LEICA MEF 4A light microscope. Fractographic analyses of surface of specimens after corrosion tests were conducted using DSM 940 Digital Scanning Microscope, with 12nm of resolving power and 15kV of accelerating voltage, supplied by OPTON Company.

3. Results and discussion

Metallographic microscopic research that was carried out permitted to observe microstructure of the sheet, rolled using thermo-mechanical processing method in accordance with the program set in Table 2 and surface of specimens put to the corrosion test in 0.5N NaCl solution. Specimens taken from rolled segment of the sheet reveal austenite microstructure with annealing twins and numerous slip bands inside the grains of γ phase (Figs. 1, 2).
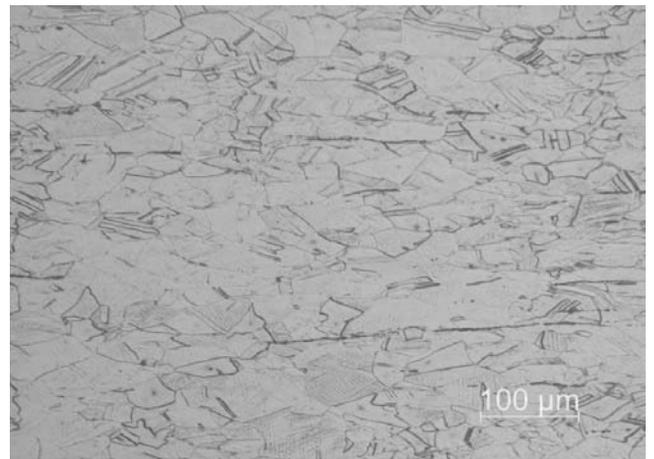

Fig. 1. Structure of the investigated steel after the thermo-mechanical processing. Austenite grains with annealing twins and slip bands apparent

Metallographic observations of sample surface after corrosion test using weight method showed numerous corrosion damages. The view of sample surface after corrosion tests in 0.5N NaCl solution carried out for 24 hours is presented in Fig. 3. Numerous micropores and pits were revealed on the surface of samples investigated in this medium (Fig. 3). Similar corrosion effects were observed on the surface of specimens after electrochemical analyses (Fig. 4).Corrosion tests carried out using weight method allowed to calculate volume loss of a sample as well as the

corrosion rate. The initial volume of the sample, V_p, was equal 0.84348 cm^3, whereas the mass of the sample before the corrosion test was equal 5.4 g. Calculated volume of the sample after the corrosion test in 0.5N NaCl solution, V_k, was equal 0.78914 cm^3, therefore its volume loss, V_u, determined using dependence (1) was equal 6.4%. Corrosion rate, determined using equation (2), was equal 0.091 g cm^{-2} day^{-1}.
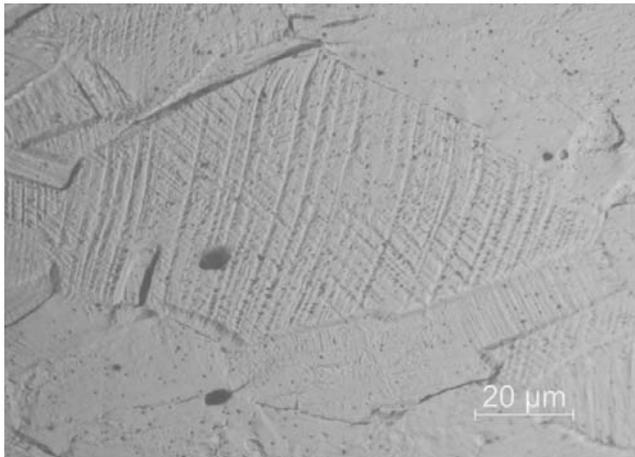

Fig. 2. Structure of the investigated steel after the thermo-mechanical processing. Austenite grains and slip bands apparent
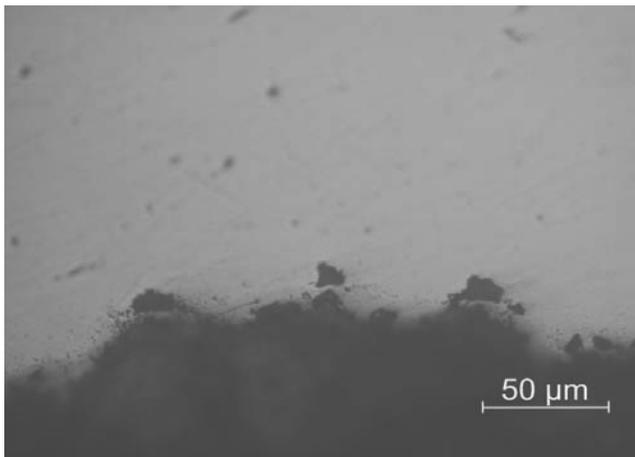
Fig. 3. Micropores and corrosion pits on a specimen surface after immersion tests in the 0.5N NaCl

Performed electrochemical analysis revealed that the open circuit potential for all the samples established itself after 400s (Fig. 5). The course of changes of current density in a function of potential for the sample investigated in 0.5N NaCl solution is presented in Fig. 6. The value of corrosion potential E_{cor} was equal -796 mV and the density of corrosion current i_{kor} determined basing on the Stern-Geary equation was equal 0.0084 mA/cm^2. Determination of pitting potential, E_b, was impossible due to the fast course of corrosion processes. In case of the sample investigated in 0.5N NaCl solution passivation did not

occur. The factors which precluded repassivation inside pits being formed on the surface of the sample were probably an increase of chloride ions concentration as a consequence of their relocation along the corrosion current, what made a contribution to the formation of a corrosion cell inside the pit as well as difficult supply of oxygen into the interior of the pit due to its low solubility in the electrolyte. The increase of the current density in positive direction on the polarization curves, what contributed to the intensification of corrosion process, was observed in case of one sample. The change of polarization of samples didn't cause any decrease of anodic current density.

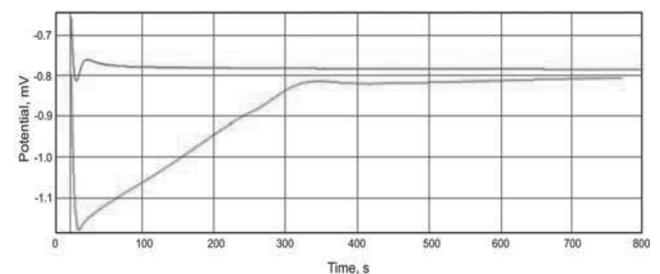Fig. 4. Micropores and corrosion pits on a specimen surface after electrochemical investigations in the 0.5N NaCl

Fig. 5. Change in the potential E_{corr} as a function of time for the specimen investigated in the 0.5N NaCl
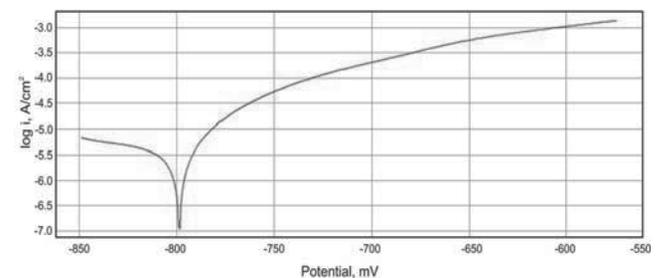

Fig. 6. Change in the current density as a function of potential for the specimen investigated in the 0.5N NaCl
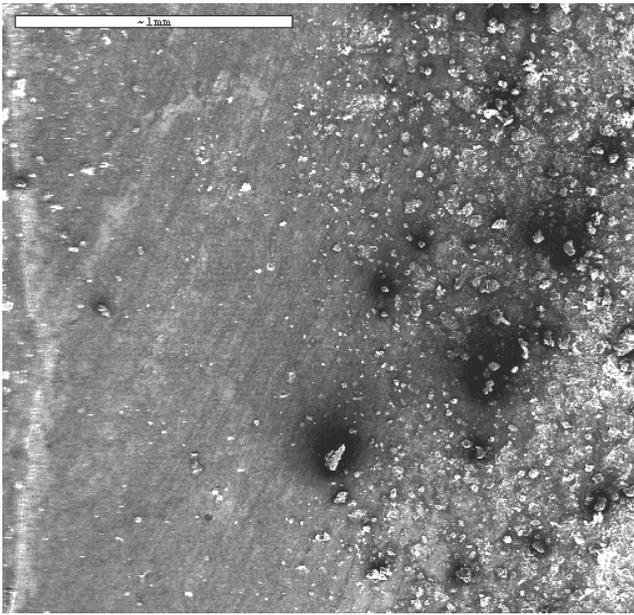
Fig. 7. Numerous, large pits on a specimen surface after immersion tests
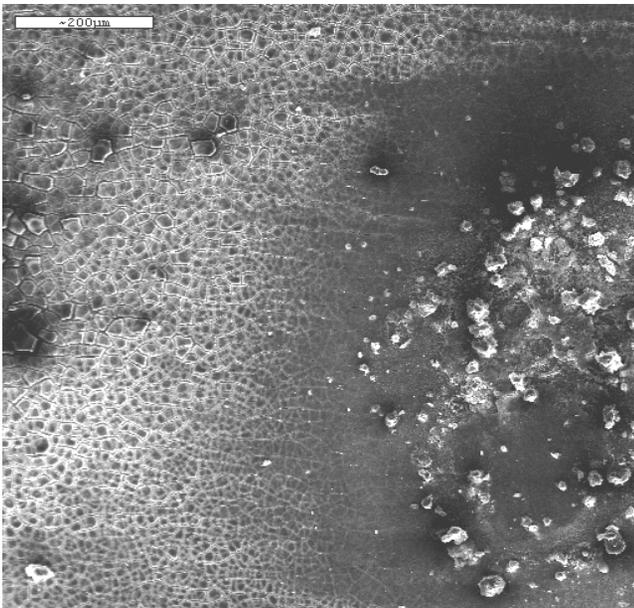

Fig. 8. Numerous pits on a specimen surface after electrochemical tests

Fractographic analyses of sample surface put to corrosion tests allowed to evaluate the type and the degree of corrosion damages. On the surface of samples investigated in 0.5N NaCl solution for 24h, numerous pits and micropores with diversified size were revealed (Figs. 7-9), however the pits present on the surface of samples coming from weight method were characterized by bigger sizes in relation to the pits observed on

samples after electrochemical analyses. Damaging of a superficial layer occurred around the pits. Cracked passive layer was also observed, what could be a result of rapid penetration of corrosive medium into interior of investigated specimens (Fig. 10). Similar corrosion products were identified on the surface of specimens after electrochemical analyses in 0.5N NaCl solution (Figs.11, 12).
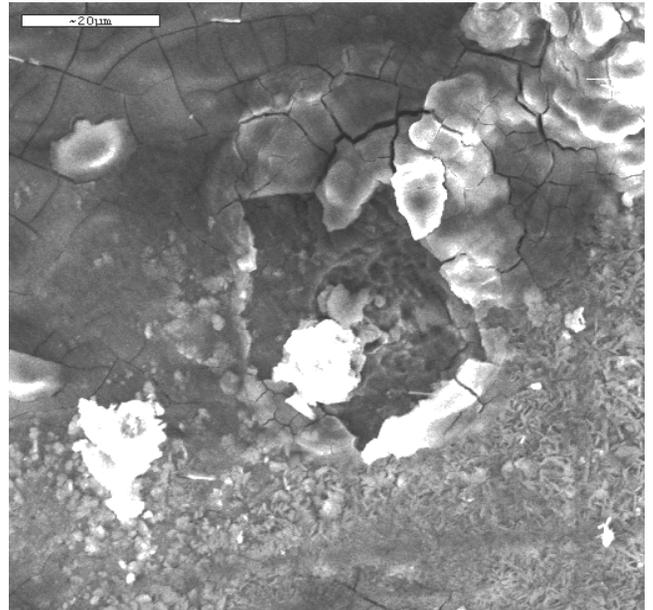

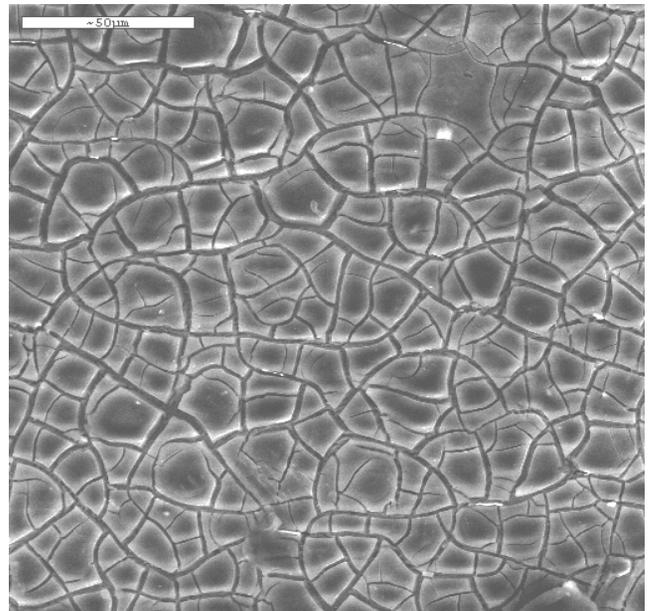Fig. 9. Corrosion pits and the partially cracked surface layer of the specimen

Fig. 10. Cracked passive layer on a surface of the specimen after immersion tests
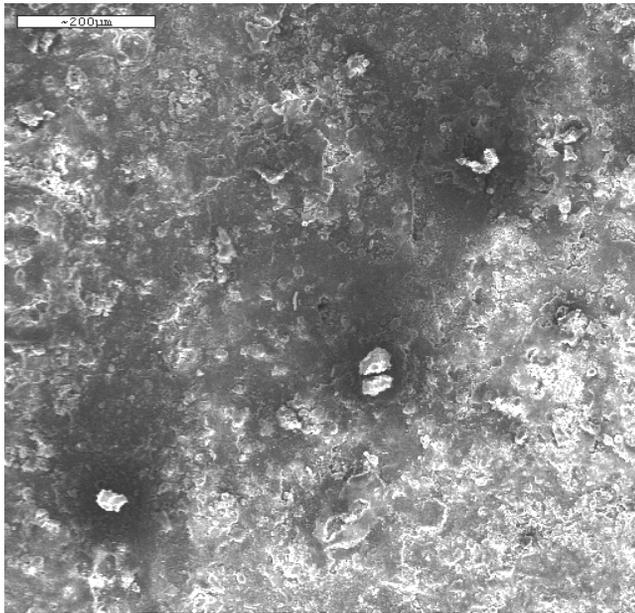
Fig. 11. Corrosion pits on a surface of the specimen after electrochemical tests
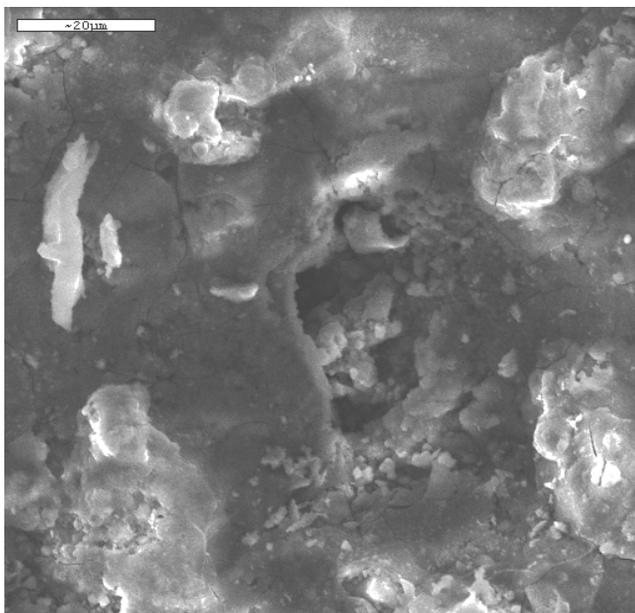

Fig. 12. A small corrosion pit on a surface of the specimen after electrochemical tests

The observed corrosion products are related to the chemical composition rather than to the phase structure of the steel. It is connected with the high dissolution rate of manganese and iron atoms in NaCl solution. Hamada et al. [21] and Zhang et al. [24] reported that the stability of Mn in high-manganese steels containing Al is low. It leads to forming unstable oxides and preferential dissolving of manganese at the oxide/electrolyte interface.

Hamada et al. [22] reported that the corrosion behaviour of Fe-Mn-Al alloys in chloride solutions can be improved by the anodic passivation in 30% HNO_3 aqueous solution. They observed that the prolonged to 5h anodic ageing leads to a modification of the chemical composition of the surface layer, connected with reducing the manganese concentration at the surface and the enrichment this region in Al, improving the corrosion resistance.

It is difficult to say, if this process can improve the corrosion resistance of the investigated steel because of lower concentration of Al compared to steels investigated by Hamada, where aluminium concentraction was about 6%. Another way of improving the corrosion resistance of high-manganese steels is to use zinc coatings. Due to alloying problems, the best solution is the use the electro-galvanizing process [21, 25].

4. Conclusions

Metallographic investigations of samples cut from the sheet produced with the thermo-mechanical processing method showed that the steel has partially recrystallized austenitic microstructure. Numerous annealing twins as well as slip bands were revealed in the microstructure of the new-developed steel.

Metallographic observations of surface of samples after corrosion tests showed numerous corrosion damages. After investigations in 0.5N NaCl solution numerous corrosion pits were revealed. The same corrosion effects were observed on samples deriving from the immersion tests and after potentiodynamic analyses. Corrosion tests carried out using weight method revealed no corrosion resistance of the steel in the chloride medium. The volume of investigated samples immersed in 0.5N NaCl solution for 24h decreased by approximately 6.5%, yet the corrosion progressed with a rate of 0.091 g $\cdot cm^{-2}$ day^{-1}.

According to the results of potentiodynamic analyses it was found that the samples of examined steel show poor corrosion resistance in the NaCl solution. The observed corrosion products are related to the chemical composition rather than to the phase structure of the steel. It is connected with the high dissolution rate of manganese and iron atoms in NaCl solution. The low stability of Mn leads to forming unstable layer and preferential dissolving of manganese at the oxide/electrolyte interface. The factors that precluded repassivation inside the pit were probably an increase of chloride ions, which made a contribution to the formation of a corrosion cell inside the pit and difficult supply of oxygen into the interior of the pit due to its low solubility in the electrolyte.

Conducted fractographic analyses of samples after corrosion tests revealed corrosion products on their surface in a form of pits with diversified size. Damaging of a superficial layer has occurred around the pits. Moreover, cracked passivation layer allowing further penetration of the corrosive medium was observed.

References

[1] H. Takechi, Application of IF based sheet steels in Japan, Proceedings of the International Conference on the Processing, Microstructure and Properties of IF Steels, Pittsburgh, 2000, 1-12.

[2] A.D. Paepe, J.C. Herman, Improved deep drawability of IF-steels by the ferrite rolling practice, Proceedings of the 37th Mechanical Working and Steel Processing Conference, Baltimore, 1999, 951-962.

[3] J. Adamczyk, A. Grajcar, Heat treatment and mechanical properties of low-carbon steel with dual-phase microstructure, Journal of Achievements in Materials and Manufacturing Engineering 22/1 (2007) 13-20.

[4] A. Grajcar, Hot-working in the $\gamma+\alpha$ region of TRIP-aided microalloyed steel, Archives of Materials Science and Engineering 28/12 (2007) 743-750.

[5] E. Doege, S. Kulp, Ch. Sunderkötter, Properties and application of TRIP-steel in sheet metal forming, Steel Research 73 (2002) 303-308.

[6] S. Ganesh Sundara Raman, K.A. Padmanabhan, Tensile deformation-induced martensitic transformation in AISI 304LN austenitic stainless steel, Journal of Materials Science Letters 13 (1994) 389-392.

[7] G. Frommeyer, U. Brüx, P. Neumann, Supra-ductile and high-strength manganese-TRIP/TWIP steels for high energy absorption purposes, ISIJ International 43 (2003) 438-446.

[8] S. Allain, J.P. Chateau, O. Bouaziz, S. Migot, N. Guelton, Correlations between the calculated stacking fault energy and the plasticity mechanisms in Fe-Mn-C alloys, Materials Science and Engineering A 387-389 (2004) 158-162.

[9] O. Grässel, L. Krüger, G. Frommeyer, L.W. Meyer, High strength Fe-Mn-(Al, Si) TRIP/TWIP steels development – properties – application, International Journal of Plasticity 16 (2000) 1391-1409.

[10] S. Vercammen, B. Blanpain, B.C. De Cooman, P. Wollants, Mechanical behaviour of an austenitic Fe-30Mn-3Al-3Si and the importance of deformation twinning, Acta Materialia 52 (2004) 2005-2012.

[11] G. Frommeyer, O. Grässel, High strength TRIP/TWIP and superplastic steels: development, properties, application, La Revue de Metallurgie-CIT 10 (1998) 1299-1310.

[12] S. Allain S, J-P. Chateau, D. Dahmoun, O. Bouaziz, Modeling of mechanical twinning in a high manganese content austenitic steel, Materials Science and Engineering A 387-389 (2004) 272-277.

[13] B.X. Huang, X.D. Wang, Y.H. Rong, L. Wang, L. Jin, Mechanical behavior and martensitic transformation of an Fe-Mn-Si-Al-Nb alloy, Materials Science and Engineering A 438-440 (2006) 306-313.

[14] L.A. Dobrzański, A. Grajcar, W. Borek, Influence of hot-working conditions on a structure of high-manganese austenitic steels, Journal of Achievements in Materials and Manufacturing Engineering 29/1 (2008) 139-142.

[15] A. Grajcar, M. Opiela, G. Fojt-Dymara, The influence of hot-working conditions on a structure of high-manganese steel, The 1st International Lower Silesia – Saxony Conference – Advanced Metal Forming Processes in Automotive Industry, Wrocław, 2008, 213-221.

[16] L.A. Dobrzański, A. Grajcar, W. Borek, Hot-working behaviour of high-manganese austenitic steels, Journal of Achievements in Materials and Manufacturing Engineering 31/1 (2008) 7-14.

[17] L.A. Dobrzański, A. Grajcar, W. Borek, Microstructure evolution and phase composition of high-manganese austenitic steels, Journal of Achievements in Materials and Manufacturing Engineering 31/1 (2008) 218-225.

[18] Y.G. Kim, Y.S. Park, J.K. Han, Low temperature mechanical behavior of microalloyed and controlled-rolled Fe-Mn-Al-C-X alloys, Metallurgical and Materials Transactions 16A (1985) 1689-1693.

[19] C.J. Altstetter, A.P. Bentley, J.W. Fourine, A.N. Kirkbride, Processing and properties of Fe-Mn-Al alloys, Materials Science and Engineering A82 (1986) 13-25.

[20] I.M. Ghayad, A.S. Hamada, N.N. Girgis, W.A. Ghanem, Effect of cold working on the aging and corrosion behaviour of Fe-Mn-Al stainless steel, Steel Grips 4 (2006) 133-137.

[21] A.S. Hamada, Manufacturing, mechanical properties and corrosion behavioiur of high-Mn TWIP steels, Acta Universitatis Ouluensis C281 (2007) 1-51.

[22] A.S. Hamada, L.P. Karjalainen, M.A. El-Zeky, Effect of anodic passivation on the corrosion behaviour of Fe-Mn-Al steels in 3.5%NaCl, Proceedings of the 9th International Symposium on the Passivation of Metals and Semiconductors and the Properties of ThinOxide Layers, Paris, 2005, 77-82.

[23] J. Baszkiewicz, M. Kamiński, Fundamentals of materials corrosion, The Warsaw University of Technology Publishers, Warsaw, 1997 (in Polish).

[24] Y.S. Hang, X.M. Zhu, M. Liu, R.X. Che, Effects of anodic passivation on the constitution, stability and resistance to corrosion of passive film formed on an Fe-24Mn-4Al-5Cr alloy, Applied Surface Science 222 (2004) 89-101.

[25] J. Inagaki, M. Sakurai, T. Watanabe, Alloying reactions in hot dip galvanizing and galvannealing processes, ISIJ International 35 (1995) 1388-1393.